

First and second sound of a unitary Fermi gas in highly elongated harmonic traps

Xia-Ji Liu¹ and Hui Hu¹

¹Centre for Quantum and Optical Science, Swinburne University of Technology, Melbourne 3122, Australia

(Dated: March 9, 2021)

Using a variational approach, we present the full solutions of the simplified one-dimensional two-fluid hydrodynamic equations for a unitary Fermi gas trapped in a highly elongated harmonic potential, which is recently derived by Stringari and co-workers [Phys. Rev. Lett. **105**, 150402 (2010)]. We calculate the discretized mode frequencies of first and second sound along the weak axial trapping potential, as a function of temperature and the form of superfluid density. We show that the density fluctuations in second sound modes, due to their coupling to first sound modes, are large enough to be measured in current experimental setups such as that exploited by Tey *et al.* at the University of Innsbruck [Phys. Rev. Lett. **110**, 055303 (2013)]. Owing to the sensitivity of second sounds on the form of superfluid density, the high precision of the measured second sound frequencies may provide us a promising way to accurately determine the superfluid density of a unitary Fermi gas, which so far remains elusive.

PACS numbers: 67.85.Lm, 03.75.Ss, 05.30.Fk

I. INTRODUCTION

Over the past few years, first and second sound of a unitary atomic Fermi gas at a broad Feshbach resonance have received increasing attentions [1–13]. Being the in-phase density oscillations (first sound) and out-of-phase temperature oscillations (second sound) [14, 15], these sound modes provide a useful probe of the equation of state [9, 10, 16–19] and superfluid density [3–7, 11, 13] of the unitary Fermi gas. The latter quantity of superfluid density is of particular interest, as it is notoriously difficult to calculate in theory. In practice, it could be measured through second sound wave propagation [5]. Indeed, in superfluid helium ⁴He, the accurate knowledge of its superfluid density, slightly below the lambda transition, is obtained by the measurement of temperature waves [20].

A strongly interacting unitary Fermi gas bears a lot of similarity to superfluid helium [4, 6]. Due to strong correlation, the first and second sound in both systems are nearly decoupled. Yet, the weak coupling between sounds still leads to a sizable hybridization effect and hence a measurable density fluctuation for second sound. This gives rise to a promising way of exciting and detecting second sound through density measurements in a unitary Fermi gas [5, 6]. For an isotropically trapped unitary Fermi gas, such a hybridization effect has been analyzed by Taylor *et al.*, using the standard dissipationless Landau two-fluid hydrodynamic approach [4]. Experimentally, however, it is more feasible to confine a unitary Fermi gas in highly elongated traps. For this configuration, the viscosity and thermal conductivity terms in the two-fluid hydrodynamic equations become important and enable a simplified one-dimensional (1D) hydrodynamic description, as suggested by Bertaina, Pitaevskii and Stringari [8]. In a recent milestone experiment, a second sound wave has been excited in a highly elongated unitary Fermi gas, and its propagation along the weakly confined axial axis has been measured [11]. The

simplified 1D hydrodynamic equations has been used to extract the superfluid density from the resulting second sound velocity data. Unfortunately, at present the experimental accuracy of sound velocity is not enough to give a satisfactory determination of superfluid density [11].

In this paper, we propose that the measurement of *discretized* mode frequencies of low-lying second sound along the weakly confined axial direction may provide an accurate means of determining superfluid density. Indeed, the latest measurement of discretized first sound mode frequencies [9] indicates a very small relative error ($\sim 0.5\%$), which is at least an order smaller in magnitude than the relative error in sound velocity data [11].

For this purpose, we fully solve the coupled 1D hydrodynamic equations in the presence of a weak axial harmonic potential, and obtain the density fluctuations of discretized low-lying second sound modes, which arise from their coupling to first sound modes. We find that these density fluctuations are significant, thereby making second sound modes observable in current experiments, by modulating, for example, the weakly confined axial trapping potential. Our full solutions of the simplified 1D hydrodynamic equations complement the earlier results obtained by Hou, Pitaevskii and Stringari [12], where the decoupled first and second sound mode frequencies are calculated with simple variational ansatz for displacement fields. In this work, we emphasize the correction to discretized mode frequencies, due to the weak coupling between first and second sound.

The rest of paper is organized as follows. In the next section, we briefly outline the reduced 1D thermodynamics, as an input for the simplified 1D hydrodynamic description. In Sec. III, we show how to solve the coupled 1D hydrodynamic equations by using a variational approach. In Sec. IV, we first provide results for the decoupled first and second sound solutions and then present the density fluctuations of some low-lying second sound modes. Finally, in Sec. V we draw our conclusion and briefly describe how to obtain the superfluid density of

a unitary Fermi gas from the measured low-lying second sound mode frequencies.

II. 1D REDUCED THERMODYNAMICS

We consider a unitary Fermi gas trapped in highly anisotropic harmonic potential,

$$V_{ext}(r_{\perp}, z) = \frac{1}{2}m\omega_{\perp}^2 r_{\perp}^2 + \frac{1}{2}m\omega_z^2 z^2, \quad (1)$$

with atomic mass m and trapping frequency $\omega_z \ll \omega_{\perp}$. We assume that the number of atoms in the Fermi cloud, typically of $N \sim 10^5$ in current experiments, is large enough, so that we can safely use the local density approximation and treat the atoms in the position (r_{\perp}, z) as uniform matter with a local chemical potential $\mu(r_{\perp}, z) = \mu - V_{ext}(r_{\perp}, z)$, where μ is the chemical potential at the trap center. In this way, we may write the local pressure and number density in the form,

$$P(r_{\perp}, z) = \frac{k_B T}{\lambda_T^3} f_p^{3D} \left[\frac{\mu(r_{\perp}, z)}{k_B T} \right], \quad (2)$$

$$n(r_{\perp}, z) = \frac{1}{\lambda_T^3} f_n^{3D} \left[\frac{\mu(r_{\perp}, z)}{k_B T} \right], \quad (3)$$

where $\lambda_T \equiv \sqrt{2\pi\hbar^2/(mk_B T)}$ is the thermal wavelength at temperature T , $f_p^{3D}(t)$ and $f_n^{3D}(t) = df_p^{3D}(t)/dt$ are two universal functions satisfied by a unitary Fermi gas due to its universal thermodynamics [21–28].

It was shown by Bertaina, Pitaevskii and Stringari [8] that, with tight radial confinement, the standard Landau two-fluid hydrodynamic equations defined in three dimensions can be greatly simplified. The key observation is that, as a direct consequence of the dissipation terms (i.e., nonzero viscosity and thermal conductivity), the local fluctuations in temperature and chemical potential become essentially independent on the radial coordinates, if we are interested in the low-energy excitations at frequency $\omega_z \ll \omega_{\perp}$. Therefore, we could integrate out the radial degree of freedom in thermodynamic variables and derive 1D reduced thermodynamics [12]. In particular, we may obtain a reduced Gibbs-Duhem relation,

$$\delta P_1 = s_1 \delta T + n_1 \delta \mu, \quad (4)$$

where the variables P_1 , s_1 and n_1 are the radial integrals of their three-dimensional counterparts, namely the local pressure, entropy density and number density. For example, we have [12],

$$P_1(z) \equiv \int dr_{\perp} 2\pi r_{\perp} P(r_{\perp}, z) = \frac{2\pi(k_B T)^2}{m\omega_{\perp}^2 \lambda_T^3} f_p(x), \quad (5)$$

where

$$x \equiv \left(\mu - \frac{1}{2}m\omega_z^2 z^2 \right) / k_B T \quad (6)$$

and we have introduced the universal scaling function,

$$f_p(x) \equiv \int_0^{\infty} dt f_p^{3D}(x-t). \quad (7)$$

All the 1D thermodynamic variables can then be derived from the reduced Gibbs-Duhem relation, such as [12]

$$n_1(z) = \left(\frac{\partial P_1}{\partial \mu} \right)_T = \frac{2\pi k_B T}{m\omega_{\perp}^2 \lambda_T^3} f_n(x), \quad (8)$$

$$s_1(z) = \left(\frac{\partial P_1}{\partial T} \right)_{\mu} = \frac{2\pi k_B T}{m\omega_{\perp}^2 \lambda_T^3} \left[\frac{7}{2} f_p(x) - x f_n(x) \right], \quad (9)$$

where $f_n(x) \equiv df_p(x)/dx = f_p^{3D}(x)$ according to Eq. (7). Furthermore, it is straightforward to obtain the specific heats per particle at constant linear density and pressure [12],

$$\bar{c}_{v1}(z) = T \left(\frac{\partial \bar{s}_1}{\partial T} \right)_{n_1} = \frac{35}{4} \frac{f_p(x)}{f_n(x)} - \frac{25}{4} \frac{f_n(x)}{f_n'(x)}, \quad (10)$$

$$\bar{c}_{p1}(z) = T \left(\frac{\partial \bar{s}_1}{\partial T} \right)_{P_1} = \bar{c}_{v1} \frac{7}{5} \frac{f_p(x) f_n'(x)}{f_n^2(x)}, \quad (11)$$

where $\bar{s}_1 \equiv s_1/(n_1 k_B)$ is the entropy per particle and $f_n'(x) \equiv df_n(x)/dx = f_n^{3D}(x)$. It is also easy to check the universal relations,

$$n_1 \left(\frac{\partial P_1}{\partial n_1} \right)_{\bar{s}_1} = \frac{7}{5} P_1, \quad (12)$$

$$\left(\frac{\partial P_1}{\partial s_1} \right)_{n_1} = \frac{2}{5} T. \quad (13)$$

For the local superfluid density, similarly we express it by a universal function f_s^{3D} :

$$n_s(r_{\perp}, z) = \frac{1}{\lambda_T^3} f_s^{3D} \left[\frac{\mu(r_{\perp}, z)}{k_B T} \right]. \quad (14)$$

By integrating out the radial coordinate, we find the expression

$$n_{s1}(z) = \int dr_{\perp} 2\pi r_{\perp} n_s(r_{\perp}, z) = \frac{2\pi k_B T}{m\omega_{\perp}^2 \lambda_T^3} f_s(x), \quad (15)$$

where the universal scaling function $f_s(x)$ is defined by,

$$f_s(x) = \int_0^{\infty} dt f_s^{3D}(x-t). \quad (16)$$

The universal function $f_p^{3D}(t)$ or $f_n^{3D}(t)$ of a homogeneous unitary Fermi gas, where $t \equiv \mu/k_B T$, has been measured by the MIT team with high precision [28], both below and above the critical temperature for superfluid phase transition. In Fig. 1, we show the 1D universal scaling functions, calculated by using the experimental MIT data for $f_n^{3D}(t)$, which has been smoothly extrapolated to both low and high temperature regimes where

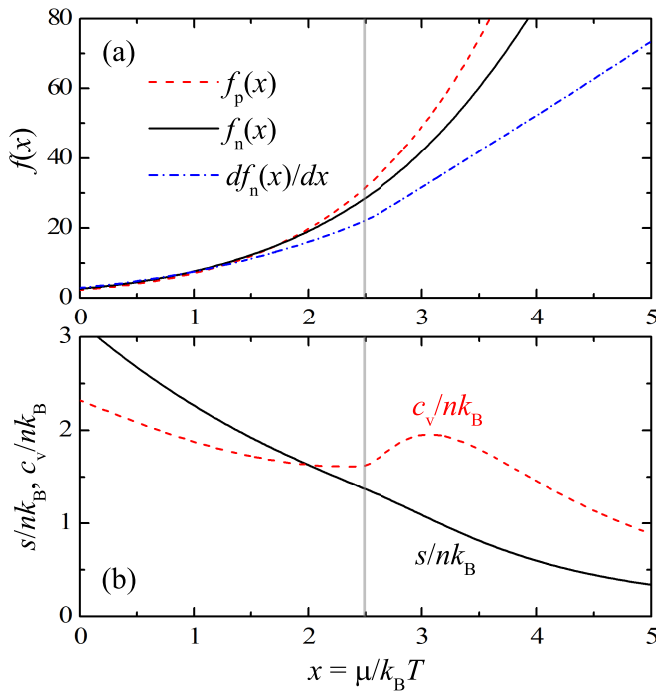


FIG. 1: (Color online) (a) 1D universal scaling functions $f_p(x)$, $f_n(x)$ and $df_n(x)/dx$ as a function of the dimensionless variable $x = \mu/(k_B T)$. (b) 1D entropy $\bar{s} = s/(nk_B)$ and specific heat per particle $\bar{c}_v = c_v/(nk_B)$ as a function of $x = \mu/(k_B T)$. The vertical grey lines indicate the critical threshold for superfluidity, $x_c \simeq 2.49$ [28].

the behavior of $f_n^{3D}(t)$ is known [6, 12, 29, 30]. Hereafter, without any confusion, we drop the subscript “1” in all the 1D thermodynamic variables.

In contrast, the universal function for superfluid density $f_s^{3D}(t)$ remains elusive [3, 7, 31]. In this work, we will use a phenomenological ansatz for the three-dimensional superfluid fraction $(n_s/n)^{3D} = f(T/T_c)$, following the strategy used in Ref. [12]. Thus, recalling that $T/T_c = [f_n^{3D}(t)/f_n^{3D}(t_c \simeq 2.49)]^{-2/3}$, the universal function $f_s^{3D}(t)$ is given by,

$$f_s^{3D}(t) = f_n^{3D}(t) f \left\{ \left[\frac{f_n^{3D}(t)}{f_n^{3D}(t_c \simeq 2.49)} \right]^{-2/3} \right\}. \quad (17)$$

In the following, we will use the phenomenological superfluid fraction [12]

$$f \left(\frac{T}{T_c} \right) = 1 - \left(\frac{T}{T_c} \right)^4, \quad (18)$$

unless otherwise stated.

III. 1D SIMPLIFIED TWO-FLUID HYDRODYNAMIC EQUATIONS

Using 1D thermodynamic variables in the standard Landau two-fluid hydrodynamic description [15], it is

straightforward to write down the simplified 1D two-fluid hydrodynamic equations. As discussed in the previous work [1, 3, 4, 12], the solutions of these equations with frequency ω at temperature T can be derived by minimizing a variational action, which, in terms of displacement fields $u_s(z)$ and $u_n(z)$, is given by,

$$S^{(2)} = \frac{1}{2} \int dz \left[m\omega^2 (n_s u_s^2 + n_n u_n^2) - \left(\frac{\partial \mu}{\partial n} \right)_s (\delta n)^2 - 2 \left(\frac{\partial T}{\partial n} \right)_s \delta n \delta s - \left(\frac{\partial T}{\partial s} \right)_n (\delta s)^2 \right]. \quad (19)$$

Here, $n_s(z)$ and $n_n(z) = n(z) - n_s(z)$ are the reduced 1D superfluid and normal-fluid densities. $\delta n(z) \equiv -\partial(n_s u_s + n_n u_n)/\partial z$ and $\delta s(z) \equiv -\partial(s u_n)/\partial z$ are the density and entropy fluctuations, respectively. The effect of the weak axial trapping potential $V_{ext}(z) = m\omega_z^2 z^2/2$ enters Eq. (19) via the position dependence of the equilibrium thermodynamic variables, within the local density approximation.

In superfluid helium, the solutions of the hydrodynamic action Eq. (19) can be well classified as density and temperature waves, which are the pure in-phase mode with $u_s = u_n$ and the pure out-of-phase mode with $n_s u_s + n_n u_n = 0$, referred to as first and second sound, respectively [15]. We may use the similar characterization for a unitary Fermi gas. To this aim, it is useful to rewrite the action Eq. (19) in terms of the displacement fields $u_a = (n_s u_s + n_n u_n)/n$ and $u_e = u_s - u_n$, since the density and temperature fluctuations can be expressed by $\delta n = -\partial(n u_a)/\partial z$ and $\delta T = (\partial T/\partial s)_n \partial(s n_s u_e/n)/\partial z$, respectively. Making use of standard thermodynamic identities, we find that

$$S^{(2)} = \frac{1}{2} \int dz \left[\mathcal{S}^{(a)} + \mathcal{S}^{(e)} + \mathcal{S}^{(ae)} \right], \quad (20)$$

where

$$\mathcal{S}^{(a)} = m(\omega^2 - \omega_z^2) n u_a^2 - n \left(\frac{\partial P}{\partial n} \right)_s \left(\frac{\partial u_a}{\partial z} \right)^2, \quad (21)$$

$$\mathcal{S}^{(e)} = m\omega^2 \frac{n_s n_n}{n} u_e^2 - \left(\frac{\partial T}{\partial s} \right)_n \left[\frac{\partial}{\partial z} \left(\frac{s n_s}{n} u_e \right) \right]^2, \quad (22)$$

$$\mathcal{S}^{(ae)} = 2 \left(\frac{\partial P}{\partial s} \right)_n \frac{\partial u_a}{\partial z} \frac{\partial}{\partial z} \left(\frac{s n_s}{n} u_e \right). \quad (23)$$

In the absence of the coupling term $\mathcal{S}^{(ae)}$, it is clear that the first sound mode, describe by $\mathcal{S}^{(a)}$, is the exact solution for pure density oscillations (i.e., $u_e = 0$ or $\delta T = 0$), while the second sound mode given by $\mathcal{S}^{(e)}$ corresponds to pure temperature oscillations with $u_a = 0$ or $\delta n = 0$. For a uniform superfluid ($V_{ext} = 0$), the solutions of $\mathcal{S}^{(a)}$ and $\mathcal{S}^{(e)}$ are plane waves of wave vector q with dispersion $\omega_1 = c_1 q$ and $\omega_2 = c_2 q$, where $mc_1^2 = (\partial P/\partial n)_s$ and

$$mc_2^2 = k_B T \frac{\bar{s}^2 n_s}{\bar{c}_v n_n}. \quad (24)$$

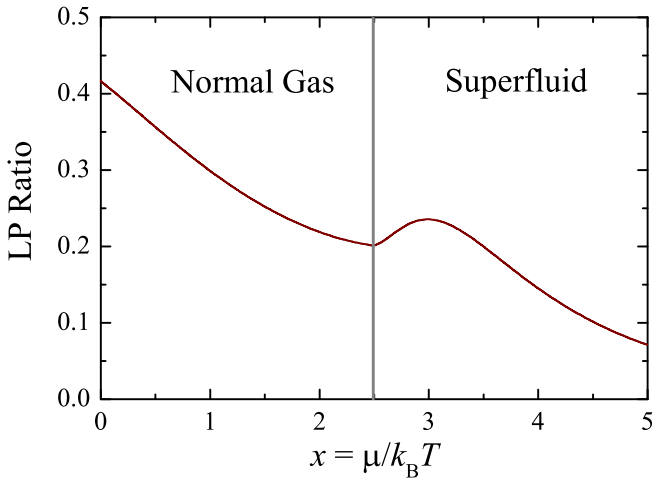


FIG. 2: (Color online) Landau-Placzek parameter ϵ_{LP} as a function of $x = \mu/(k_B T)$ in a highly elongated unitary Fermi gas.

These first and second sound velocities are the standard results used to describe superfluid helium [15].

In general, the coupling term $\mathcal{S}^{(ae)}$ is nonzero. Actually, in our case, as $(\partial P/\partial s)_n = 2T/5$, the first and second sound are necessarily coupled at any finite temperature. This coupling can be conveniently characterized by the dimensionless Landau-Placzek (LP) parameter $\epsilon_{\text{LP}} \equiv \gamma - 1$ [6], where $\gamma \equiv \bar{c}_p/\bar{c}_v$ is the ratio between the specific heats per particle at constant pressure and density. Indeed, with the coupling term, the second sound velocity c_2 may be well approximated by [6, 12]

$$mc_2^2 = k_B T \frac{\bar{s}_2^2 n_s}{\bar{c}_p n_n}, \quad (25)$$

which differs with Eq. (24) by a factor of $\gamma = \bar{c}_p/\bar{c}_v$. Thus, the LP ratio is a useful parameter to estimate the coupling between first and second sound.

In superfluid helium, $\bar{c}_p \simeq \bar{c}_v$ or $\epsilon_{\text{LP}} \simeq 0$, indicating that the first and second sound are well decoupled. For a unitary Fermi gas in highly elongated traps, we have calculated the LP ratio using the 1D thermodynamic data. As shown in Fig. 2, the ratio is less than 1/4 in the whole superfluid phase. Therefore, similar to superfluid liquid helium, the solutions of two-fluid hydrodynamic equations for a highly elongated unitary Fermi gas are well approximated as weakly coupled first and second sound modes.

We note that, in the presence of axial harmonic traps ($V_{\text{ext}} \neq 0$), the actions $\mathcal{S}^{(a)}$ and $\mathcal{S}^{(e)}$ have been solved analytically by Hou, Pitaevskii and Stringari using simple variational ansatz [12]. The coupling between first and second sound due to $\mathcal{S}^{(ae)}$ has also been briefly commented. In this work, by presenting the full variational calculations, we will show how the low-lying second sound modes are affected by the coupling. In particular, we focus on the density fluctuations of second sound modes, which are the key observable in real experiments [9].

A. Variational approach

We assume the following polynomial ansatz for the displacement fields:

$$u_a(z) = \sum_{i=0}^{N_p-1} A_i \tilde{z}^i, \quad (26)$$

$$u_e(z) = \sum_{i=0}^{N_p-1} B_i \tilde{z}^i, \quad (27)$$

where the number of the variational parameters $\{A_i, B_i\}$ is $2N_p$, and $\tilde{z} \equiv z/Z_F$ is the dimensionless coordinate with Z_F being the Thomas-Fermi radius along the weakly confined axial direction. Inserting this ansatz into the action Eq. (20), the mode frequencies are obtained by minimizing the resulting expression with respect to the $2N_p$ parameters. The precision of our variational calculations can be improved by increasing the value of N_p .

In greater detail, it is easy to see that, the action is given by

$$S^{(2)} = \frac{1}{2} \Lambda^\dagger \mathcal{S}(\omega) \Lambda, \quad (28)$$

where $\Lambda \equiv [A_0, B_0, \dots, A_i, B_i, \dots, A_{N_p-1}, B_{N_p-1}]^T$ and $\mathcal{S}(\omega)$ is a $2N_p \times 2N_p$ matrix with block elements,

$$[\mathcal{S}(\omega)]_{ij} \equiv \begin{bmatrix} M_{ij}^{(a)} \omega^2 - K_{ij}^{(a)} & -K_{ij}^{(ae)} \\ -K_{ji}^{(ae)} & M_{ij}^{(e)} \omega^2 - K_{ij}^{(e)} \end{bmatrix}. \quad (29)$$

Here, we have introduced the weighted mass moments,

$$M_{ij}^{(a)} = m \int dz \tilde{z}^{i+j} n(z), \quad (30)$$

$$M_{ij}^{(e)} = m \int dz \tilde{z}^{i+j} \left[\frac{n_s n_n}{n} \right] (z), \quad (31)$$

and the spring constants,

$$K_{ij}^{(a)} = \frac{7}{5} ij \int dz \tilde{z}^{i+j} P(z) / z^2 + \omega_z^2 M_{ij}^{(a)}, \quad (32)$$

$$K_{ij}^{(ae)} = \frac{2T}{5} i(i-1) \int dz \tilde{z}^{i+j} z^{-2} \left[\frac{sn_s}{n} \right] (z), \quad (33)$$

$$K_{ij}^{(e)} = \int dz \left(\frac{\partial T}{\partial s} \right)_n \frac{\partial}{\partial z} \left(\frac{sn_s \tilde{z}^i}{n} \right) \frac{\partial}{\partial z} \left(\frac{sn_s \tilde{z}^j}{n} \right). \quad (34)$$

In deriving $K_{ij}^{(a)}$ and $K_{ij}^{(ae)}$, we have used the universal relations satisfied by the highly elongated unitary Fermi gas: $n(\partial P/\partial n)_{\bar{s}} = 7P/5$ and $(\partial P/\partial s)_n = 2T/5$. For a given value of $\mu/k_B T$ (or T/T_F , see below), the weighted mass moments and spring constants can be calculated by using local thermodynamic variables in Eqs. (5), (8), (9), (10) and (15). We note that the universal scaling function for superfluid density is given by Eqs. (16), (17) and (18).

In practice, the minimization of the action $S^{(2)}$ is equivalent to solving

$$S(\omega)\Lambda = 0. \quad (35)$$

Once a solution (i.e., the k -th mode frequency ω_k and the coefficient eigenvector Λ_k) is found, we calculate the density fluctuation of the mode, by using

$$\delta n_k(z) = - \sum_{i=0}^{N_p-1} A_i^{(k)} \frac{\partial}{\partial z} [n(z) \tilde{z}^i]. \quad (36)$$

IV. RESULTS AND DISCUSSIONS

We have performed numerical calculations for the number of the variational parameter N_p up to 24, for any given temperature T/T_F or chemical potential $\mu/k_B T$. By recalling that the Fermi temperature T_F of a three-dimensional trapped Fermi gas is given by

$$k_B T_F = \hbar (3N\omega_z^2)^{1/3} \quad (37)$$

and the number of atoms $N = \int dz n(z)$, these two parameters are related by,

$$\frac{T}{T_F} = \left[\frac{3}{\sqrt{\pi}} \int_0^\infty dt \frac{1}{\sqrt{t}} f_n\left(\frac{\mu}{k_B T} - t\right) \right]^{-1/3}. \quad (38)$$

In the following, we first discuss the decoupled first and second sound, in connection with the previous results by Hou, Pitaevskii and Stringari [12]. Then, we focus on the effect of the mode coupling.

A. Decoupled first sound

In Ref. [12], the action $\mathcal{S}^{(a)}$ has been solved by using the ansatz $u_a^{k=2}(z) = A_2 z^2 + A_0$ and $u_a^{k=3}(z) = A_3 z^3 + A_1 z$ for the $k = 2$ and $k = 3$ first sound modes, respectively. Here, k is the index of a mode and counts the number of nodes ($= k + 1$) in its density fluctuation. These are the first two solutions, whose frequency varies with increasing temperature, due to the non-trivial temperature dependence of equation of state [12]. Indeed, it is easy to prove that

$$K_{ij}^{(a)} = \left[\frac{7}{5} \frac{ij}{(i+j-1)} + 1 \right] \omega_z^2 M_{ij}^{(a)}. \quad (39)$$

Thus, if $i = 0$ or $j = 0$, we have $K_{ij}^{(a)} = \omega_z^2 M_{ij}^{(a)}$. Together with the fact that $K_{i=0,j}^{(ae)} = 0$ or $K_{j=0,i}^{(ae)} = 0$, it is clear that the $k = 0$ first sound mode with variational ansatz $u_a^{k=0}(z) = A_0$ is an exact solution of the two-fluid hydrodynamic equations. In fact, it is precisely the undamped *dipole* oscillation, with invariant frequency $\omega = \omega_z$. Similarly, in the case of $i = 1$ or

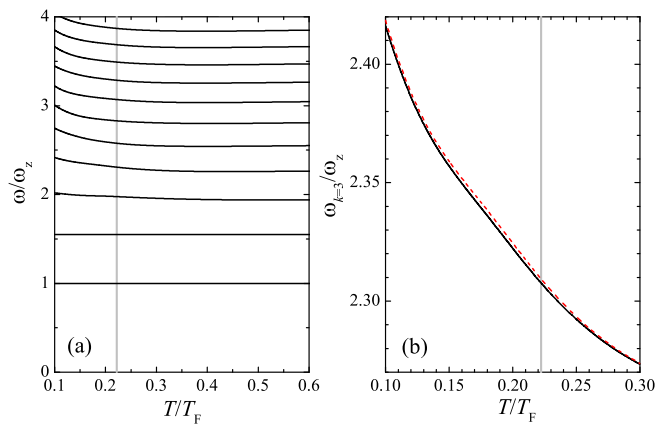


FIG. 3: (Color online) (a) Temperature dependence of the first sound mode frequencies. (b) Enlarged view for the fourth first sound mode frequency. The red dashed line shows the result with the ansatz $u_a(z) = A_3 z^3 + A_1 z$, obtained earlier by Hou, Pitaevskii and Stringari [12]. The vertical grey lines show the critical temperature, $T_c \simeq 0.223 T_F$.

$j = 1$, $K_{ij}^{(a)} = (12/5)\omega_z^2 M_{ij}^{(a)}$, revealing that the $k = 1$ first sound mode - the *breathing* mode - is another exact solution of the two-fluid hydrodynamic equation with invariant frequency $\omega = \sqrt{12/5}\omega_z$ [12, 32].

In Fig. 3(a), we report the variational results for first sound mode frequencies with $N_p = 24$. In agreement with the observation by Hou, Pitaevskii and Stringari [12], we find that $u_a^{k=2}(z)$ and $u_a^{k=3}(z)$ provide excellent variational ansatz for the third and fourth modes. As shown in Fig. 3(b), the higher-order correction, for example, for the $k = 3$ mode, is at the order of 0.1% in relative and can only be seen in the vicinity of the critical temperature.

B. Decoupled second sound

In Fig. 4(a), we present the results for the mode frequency of decoupled second sounds. With increasing temperature, the mode frequency initially increases and reaches a maximum before finally dropping to zero at the superfluid phase transition [12]. In sharp contrast to first sound modes, the convergence of the polynomial ansatz for second sound modes appears to be slow. For the lowest dipole second sound mode, our variational approach only converges at $N_p \geq 16$, as can be seen from Fig. 4(b). Moreover, compared with the fully converged result, a constant displacement field u_e (i.e., $N_p = 1$) can lead to a relative error as large as 20% close to the superfluid phase transition. For the higher order second sound modes, we observe that the convergence of the polynomial ansatz becomes even slower.

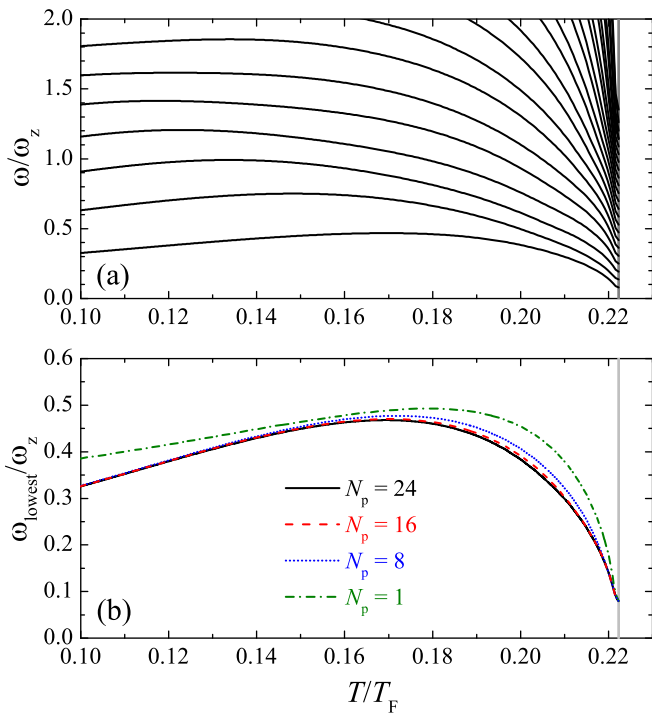


FIG. 4: (Color online) (a) Temperature dependence of the second sound mode frequencies with $N_p = 24$. The mode frequencies vanish right at superfluid phase transition. However, our numerical calculations become less accurate slightly below the transition and can not produce correctly the zero frequency exactly at T_c . (b) Enlarged view for the lowest second sound mode frequency. The mode frequency converges with increasing the number of variational ansatz N_p . The result with $N_p = 1$ (green dot-dashed line) corresponds to a constant displacement field u_e [12]. The vertical grey lines show the critical temperature.

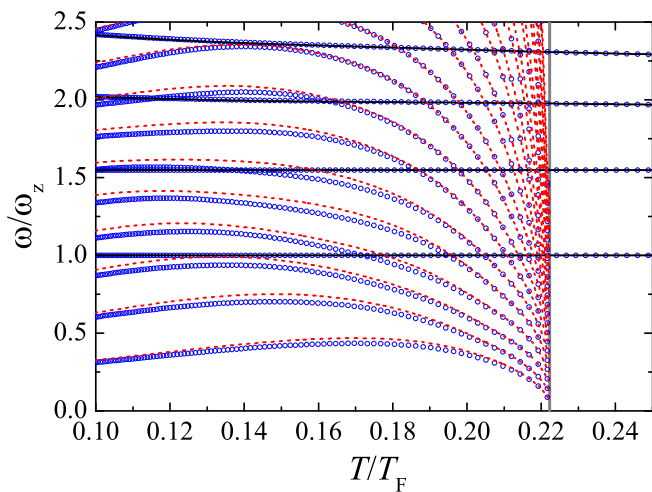


FIG. 5: (Color online) Temperature dependence of the full two-fluid hydrodynamic mode frequencies (blue circles). For comparison, we show also the mode frequencies of the decoupled first and second sounds, respectively, by black solid and red dashed lines. The vertical grey line indicates the critical temperature.

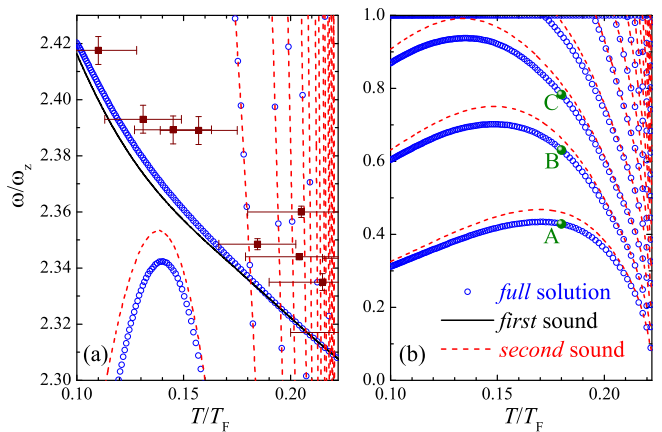


FIG. 6: (Color online) Blow-up of the full two-fluid hydrodynamic mode frequencies (blue circles), near the $k = 3$ first sound mode (a) and the lowest second sound modes (b). In (a), the experimental data from the Innsbruck experiment [9] are shown by brown solid squares with error bars.

C. Full solutions of 1D two-fluid hydrodynamics

We now include the mode coupling term $\mathcal{S}^{(ae)}$. In Fig. 5, we report the full variational results with $N_p = 24$ by blue circles. For comparison, we show also the decoupled first and second sound mode frequencies, by using black lines and red dashed lines. As anticipated, at the qualitative level, the full variational predictions can be well approximated by the decoupled results, confirming our previous idea that in highly elongated harmonic traps, the solutions of two-fluid hydrodynamics of a unitary Fermi gas can indeed be viewed as weakly coupled first and second sound modes.

At the *quantitative* level, the first sound mode is nearly unaffected by the coupling term $\mathcal{S}^{(ae)}$. This is evident in Fig. 6(a), where we present an enlarged view for the $k = 3$ first sound mode. The mode frequency has been pushed up by about 0.5% at $T \sim 0.15T_F$ by the coupling. Experimentally, the frequency of the $k = 3$ first sound mode has been measured very recently [9, 10]. In the figure, we show the experimental data by solid squares with error bars. It is known that the data systematically lie above the variational result with $u_a^{k=3}(z)$ [9, 10, 12]. Our full variational predictions seem to agree better with the experimental data. However, the improvement is too slight to account for the discrepancy.

On the other hand, the frequency of second sound modes is notably pushed down by the coupling, as shown in Fig. 6(b). The maximum correction is up to 10% when the temperature is about $0.15T_F$. Therefore, for a quantitative prediction of second sound modes over the whole temperature regime, we must fully solve the coupled Landau two-fluid hydrodynamic equations.

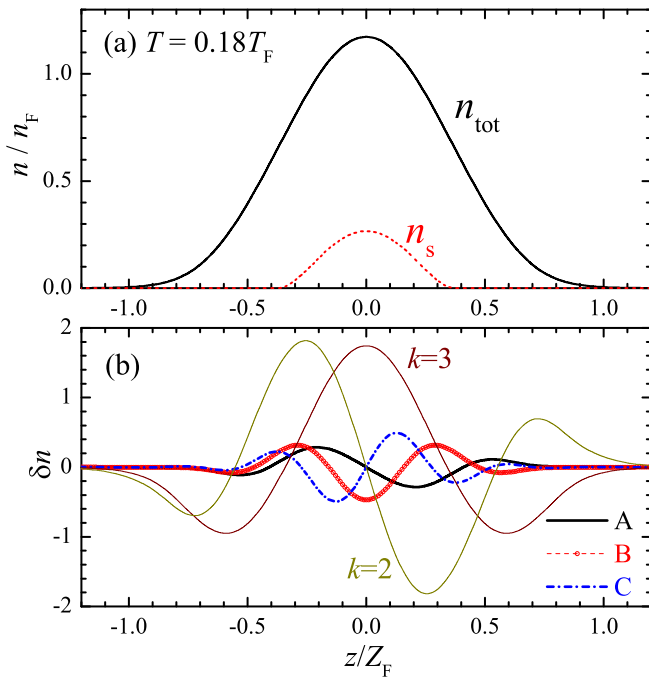


FIG. 7: (Color online) (a) Density distribution (solid line) and superfluid density distribution (dashed line) at $T = 0.18T_F$, in units of the peak linear density of an ideal Fermi gas at the trap center (n_F). (b) Density fluctuations of the $k = 2$ and $k = 3$ first sound modes (thin lines) and of the three lowest second sound modes (thick lines), at the frequencies indicated in Fig. 6(b) by A, B and C. The amplitude of the second-sound density fluctuations is about 1/3 of that of the first-sound density fluctuations.

D. Density measurement of discretized second sound modes

The sizable correction in mode frequencies strongly indicates that, the density fluctuation $\delta n_k(z)$ of a second sound mode, as a result of its coupling to first sound modes, could also be significant. In Fig. 7(b), we show the density fluctuations of the lowest three second sound modes at the temperature $T = 0.18T_F$ (thick lines), in relative to the density fluctuations of the $k = 2$ and $k = 3$ first sound modes (thin lines). The absolute amplitude of density fluctuations depends on the detailed excitation scheme used in experiments.

In a recent investigation by the Innsbruck group [9, 10], the density fluctuations of the $k = 2$ and $k = 3$ first sound modes have been excited and measured, to a reasonable accuracy. For the detailed resonant excitation scheme, we refer to the experimental papers of Refs. [9] and [10]. We anticipate that the similar excitation procedure works also for second sound modes, by carefully choosing the position and size of excitation laser beam, which provide best mode matching. As shown in Fig. 7(b), it is remarkable that the amplitude of the second sound density fluctuations is at the same order as that of the $k = 2$ and $k = 3$ first sound modes, over a useful range of temper-

atures. As we shall see below from the analysis of the density response function, this implies that the low-lying second sound mode could be observed by looking at its density fluctuation, after a proper excitation.

To obtain the density response function, we consider adding a density perturbation of the form $\delta V(z, t) = \lambda f(z)e^{-i\Omega t}$ to the equilibrium two-fluid equations, where λ is the strength of the perturbation and $f(z)$ is a normalized shape function (i.e., $\int dz f^2(z) = 1$). This leads to a density fluctuation $\delta n(z, t)$ with its amplitude proportional to λ and in turn gives the response function $\chi_{nn}(\Omega; f)$ defined by

$$\lambda \chi_{nn}(\Omega; f) e^{-i\Omega t} = \int dz f(z) \delta n(z, t). \quad (40)$$

Note that in general the response function depends on the form of the perturbation $f(z)$. In greater detail, the density perturbation generates an additional term $\delta S^{(2)}$ in the two-fluid hydrodynamic action,

$$S^{(2)} = \frac{1}{2} \Lambda_\Omega^\dagger \mathcal{S}(\Omega) \Lambda_\Omega + \delta S^{(2)}, \quad (41)$$

where

$$\delta S^{(2)} = \lambda \sum_{i=0}^{N_p-1} \int dz f(z) \frac{\partial}{\partial z} [n(z) \tilde{z}^i] A_i^{(\Omega)}. \quad (42)$$

Here we have used the index “ Ω ” to distinguish Λ_Ω from the eigenvector Λ obtained by diagonalizing the action matrix Eq. (29). By introducing a vector $F = [f_0, 0, f_1, 0, \dots, f_{N_p-1}, 0]^T$, where $f_i \equiv \int dz f(z) \partial [n(z) \tilde{z}^i] / \partial z$, we obtain

$$\Lambda_\Omega = -\lambda S^{-1}(\Omega) F \quad (43)$$

by minimizing the perturbed action. Substituting this result into the expression for the density fluctuation Eq. (36), we find that,

$$\begin{aligned} \chi_{nn}(\Omega; f) &= F^\dagger S^{-1}(\Omega) F, \\ &= \sum_k \frac{Z_k}{2\omega_k} \left(\frac{1}{\Omega - \omega_k} - \frac{1}{\Omega + \omega_k} \right), \end{aligned} \quad (44)$$

where

$$Z_k = |F^\dagger \Lambda_k|^2 = \left| \int dz f(z) \delta n_k(z) \right|^2 \quad (45)$$

is the *residue* of the response function for the k -th collective mode with eigenvector Λ_k and frequency ω_k [33].

Using Eq. (45), it is clear that a sizable density fluctuation $\delta n_k(z)$ of second sound modes - as reported in Fig. 7 - implies that a significant residue in the density response for second sound can be achieved by optimizing the *unit* shape function $f(z)$ such that $f(z) \propto \delta n_k(z)$. Therefore, discrete second sound could be excited in a similar way as first sound, without imposing a large strength λ for the density perturbation $\delta V(z, t)$.

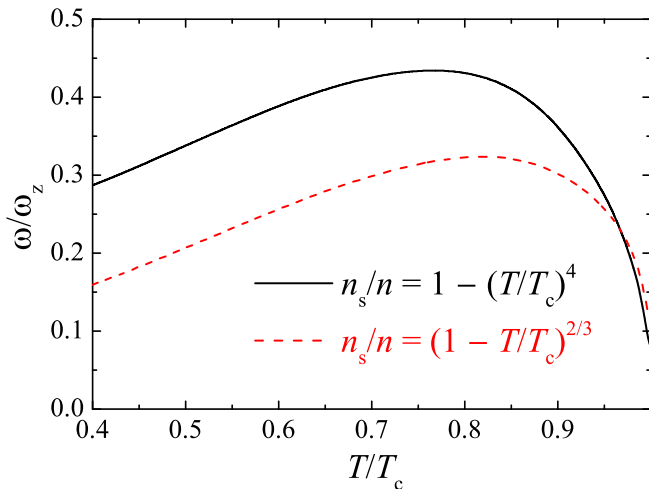


FIG. 8: (Color online) Sensitivity of the lowest second sound mode on the superfluid density. The critical temperature $T_c \simeq 0.223T_F$.

E. Dependence on the superfluid fraction

We so far restrict ourselves to the phenomenological superfluid fraction Eq. (18). In Fig. 8, we report the dependence of the lowest second sound frequency on the form of superfluid fraction. The sensitive dependence indicates that practically the unknown superfluid density of a unitary Fermi gas could be accurately determined by measuring the mode frequency of low-lying second sound modes.

V. CONCLUSIONS

In conclusion, using a variational approach, we have fully solved the one-dimensional simplified Landau two-fluid hydrodynamic equations, which describe the collective excitations of a unitary Fermi gas in highly elongated harmonic traps. Resembling the superfluid helium, the

solutions are well characterized by weakly coupled first and second sound modes. Discretized first and second sound mode frequencies have been accurately predicted.

Though the coupling between first and second sound is weak, it still induces significant density fluctuations for second sound modes, suggesting that second sound could be observed by measuring the density fluctuations after properly modulating the axial harmonic trapping potential. Owing to the very high precision in the frequency calibration, the experimental measurement of discretized second sound mode frequency provides a promising way to accurately determining the superfluid density of a unitary Fermi gas, which remains elusive to date.

Ideally, we anticipate that the relative error in the measurement of the second sound mode frequency is about 0.5%. For the low-lying modes, whose mode frequency is smaller than ω_z , the damping rate might be reasonably small. By assuming a superfluid fraction in the form,

$$f\left(\frac{T}{T_c}\right) = \left(1 - \frac{T}{T_c}\right)^{2/3} \left[a_0 + a_1 \left(\frac{T}{T_c}\right) + \dots \right], \quad (46)$$

which correctly reproduces the critical behavior near superfluid phase transition, we may determine the parameters $\{a_0, a_1, a_2, \dots\}$ by fitting the experimental data to the full variational predictions for the discretized low-lying second sound mode frequencies.

Acknowledgments

We acknowledge the useful discussion with Yan-Hua Hou, which stimulated this research. We thank Meng Khoon Tey for sending us the experimental data of the $k = 2$ and $k = 3$ first sound modes. Our work was supported by the ARC Discovery Projects (Grant Nos. DP0984637, DP140100637, DP0984522, DP140103231 and FT130100815) and NFRP-China (Grant No. 2011CB921502).

-
- [1] E. Taylor and A. Griffin, *Phys. Rev. A* **72**, 053630 (2005).
 - [2] Y. He, Q. Chen, C. C. Chien, and K. Levin, *Phys. Rev. A* **76**, 051602(R) (2007).
 - [3] E. Taylor, H. Hu, X.-J. Liu, and A. Griffin, *Phys. Rev. A* **77**, 033608 (2008).
 - [4] E. Taylor, H. Hu, X.-J. Liu, L. P. Pitaevskii, A. Griffin, and S. Stringari, *Phys. Rev. A* **80**, 053601 (2009).
 - [5] R. Watanabe, S. Tsuchiya and Y. Ohashi, *Phys. Rev. A* **82**, 043630 (2010).
 - [6] H. Hu, E. Taylor, X.-J. Liu, S. Stringari, and A. Griffin, *New J. Phys.* **12**, 043040 (2010).
 - [7] L. Salasnich, *Phys. Rev. A* **82**, 063619 (2010).
 - [8] G. Bertaina, L. P. Pitaevskii, and S. Stringari, *Phys. Rev. Lett.* **105**, 150402 (2010).
 - [9] M. K. Tey, L. A. Sidorenkov, E. R. Sánchez Guajardo, R. Grimm, M. J. H. Ku, M. W. Zwierlein, Y. H. Hou, L. Pitaevskii, and S. Stringari, *Phys. Rev. Lett.* **110**, 055303 (2013).
 - [10] E. R. Sánchez Guajardo, M. K. Tey, L. A. Sidorenkov, and R. Grimm, *Phys. Rev. A* **87**, 063601 (2013).
 - [11] L. A. Sidorenkov, M. K. Tey, R. Grimm, Y.-H. Hou, L. Pitaevskii, and S. Stringari, *Nature (London)* **498**, 78 (2013).
 - [12] Y.-H. Hou, L. P. Pitaevskii, and S. Stringari, *Phys. Rev. A* **88**, 043630 (2013).
 - [13] H. Hu and X.-J. Liu, *Phys. Rev. A* **88**, 053605 (2013).
 - [14] L. Tisza, *C. R. Phys.* **207**, 1035 (1938).
 - [15] L. D. Landau, *J. Phys. (USSR)* **5**, 71 (1941).
 - [16] S. Stringari, *Europhys. Lett.* **65**, 749 (2004).
 - [17] H. Hu, A. Minguzzi, X.-J. Liu, and M. P. Tosi, *Phys.*

- Rev. Lett. **93**, 190403 (2004).
- [18] A. Altmeyer, S. Riedl, C. Kohstall, M. J. Wright, R. Geursen, M. Bartenstein, C. Chin, J. Hecker Denschlag, and R. Grimm, Phys. Rev. Lett. **98** 040401 (2007).
- [19] J. Joseph, B. Clancy, L. Luo, J. Kinast, A. Turlapov, and J. E. Thomas, Phys. Rev. Lett. **98**, 170401 (2007).
- [20] J. G. Dash and R. D. Taylor, Phys. Rev. **105**, 7 (1957).
- [21] T.-L. Ho, Phys. Rev. Lett. **92**, 090402 (2004).
- [22] X.-J. Liu and H. Hu, Phys. Rev. A **72**, 063613 (2005).
- [23] H. Hu, X.-J. Liu, and P. D. Drummond, Europhys. Lett. **74**, 574 (2006).
- [24] H. Hu, X.-J. Liu, and P. D. Drummond, Phys. Rev. A **73**, 023617 (2006).
- [25] H. Hu, P. D. Drummond, and X.-J. Liu, Nature Phys. **3**, 469 (2007).
- [26] H. Hu, X.-J. Liu, and P. D. Drummond, Phys. Rev. A **77**, 061605 (2008).
- [27] H. Hu, X.-J. Liu, and P. D. Drummond, New J. Phys. **12**, 063038 (2010).
- [28] M. J. H. Ku, A. T. Sommer, L. W. Cheuk, and M. W. Zwierlein, Science **335**, 563 (2012).
- [29] X.-J. Liu, H. Hu, and P. D. Drummond, Phys. Rev. Lett. **102**, 160401 (2009).
- [30] X.-J. Liu, Phys. Rep. **524**, 37 (2013).
- [31] G. Baym and C. J. Pethick, Phys. Rev. A **88**, 043631 (2013).
- [32] Y.-H. Hou, L. P. Pitaevskii, and S. Stringari, Phys. Rev. A **87**, 033620 (2013).
- [33] Alternatively, we may write the residue in the form $Z_k = \left| \int dz n(z) u_a^{(k)}(z) \partial f / \partial z \right|^2$. This expression was used earlier in Ref. [4].